ACS APPLIED MATERIALS & INTERFACES

Research Article

www.acsami.org

Highly Reproducible Thermocontrolled Electrospun Fiber Based Organic Photovoltaic Devices

Taehoon Kim, Seung Jae Yang, Sae Jin Sung, Yern Seung Kim, Mi Se Chang, Haesol Jung, and Chong Rae Park*

Carbon Nanomaterials Design Laboratory, Research Institute of Advanced Materials, and Department of Materials Science and Engineering, Seoul National University, 1 Gwanak-ro, Gwanak-gu, Seoul 151-744, Korea

Supporting Information

ABSTRACT: In this work, we examined the reasons underlying the humidity-induced morphological changes of electrospun fibers and suggest a method of controlling the electrospun fiber morphology under high humidity conditions. We fabricated OPV devices composed of electrospun fibers, and the performance of the OPV devices depends significantly on the fiber morphology. The evaporation rate of a solvent at various relative humidity was measured to investigate the effects of the relative humidity during electrospinning process. The beaded nanofiber morphology of electrospun fibers was originated due to slow solvent evaporation rate under high humidity conditions. To increase the evaporation rate under high humidity conditions, warm air was applied to the electrospinning system. The beads that would have formed on the electrospun fibers were completely avoided, and the power conversion efficiencies of OPV devices fabricated under high humidity conditions could be restored. These results highlight the simplicity and effectiveness of the proposed method for improving the reproducibility of electrospun nanofibers and performances of devices consisting of the electrospun nanofibers, regardless of the relative humidity.

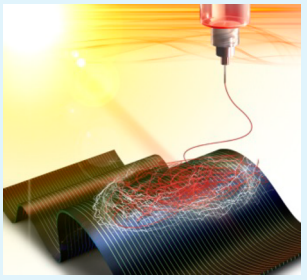

KEYWORDS: *electrospinning, photovoltaic, conjugated polymer, solar cell, nanofiber*

INTRODUCTION

Electrospinning is a facile and effective method for processing solutions into continuous fibers having diameters that can range from a few nanometers to a few micrometers.[1,2] The high aspect ratios and surface areas of electrospun fibers render them useful for a variety of applications, including membranes,[3] batteries,[4,5] and catalysts.[6] The electrospinning technique was recently applied toward the preparation of electronic devices, such as organic thin film transistors,[7,8] sensors,[9,10] and organic photovoltaic (OPV) devices[11,12] based on conjugated polymer nanofibers. One-dimensional materials with high aspect ratios have several advantages over conventional film-based materials in electronic devices: one-dimensional materials (1) form a continuous charge transport pathway,[13,14] (2) provide enhanced electrical properties,[15] and (3) offer a high surface area.[1,14] Conjugated polymer nanofibers prepared by electrospinning technique, therefore, can contribute to the preparation of high-performance devices. For OPV devices, a large surface area at the heterojunction of the electron donor and acceptor is required to facilitate the effective dissociation of electron−hole pairs, called excitons.[16] Therefore, electrospun conjugated polymer nanofibers are useful for improving the performances of OPV devices.[11,14] Moreover, the continuous shape of the electrospun fibers facilitates dissociated charge transport. Exciton dissociation and charge transport in an active layer can directly influence the photocurrent in OPV devices. Electrospun OPV devices exhibit an enhanced short-circuit current (J_{SC}) and enhanced power conversion efficiency.[12]

The reproducibility of a device is an important issue in the fabrication of OPV devices.[17,18] Because the performance of electrospun OPV devices significantly depends on diameter of the electrospun fibers,[11,12] the reproducibility of the devices is determined by the reproducibility of the electrospun fibers. However, the diameter and shape of the electrospun fibers are known to change under different atmospheric conditions, such as different temperatures and relative humidity (RH) levels.[19−22] This is an important issue in relation to electrospinning research, as reducing the humidity during a humid season is difficult. Therefore, the preparation of morphologically controlled fibers which are insusceptible to the RH should be accomplished to obtain highly reproducible devices. Otherwise, changes in the ambient conditions would induce differences in the properties of products prepared using electrospinning techniques, and this reduces the reliability of the electrospinning process as a practical fabrication procedure for various devices such as batteries, supercapacitors, sensors, and OPV devices. Although a scientific approach to manage the influence of the humidity is required, a typical solution to reduce the effect of the humidity is to build a well-designed chamber system that prevents the commercialization of electrospinning due to the high fabrication cost.

In this work, we present a simple and inexpensive process that improves the reproducibility of fibers and their photo-

Received: April 13, 2014
Accepted: February 4, 2015
Published: February 4, 2015

DOI: 10.1021/am508250q
ACS Appl. Mater. Interfaces 2015, 7, 4481−4487

voltaic performance regardless of the RH. We investigated the influence of the humidity level on the morphology of electrospun fibers and variations of the photovoltaic performances of electrospun fibers induced by morphological changes. The term, morphology, used in this work does not correspond to the morphology at the atomic level used in the OPV research field,[23,24] but rather corresponds to the shape and structure of a fiber used in the electrospinning research field. It was found that the morphology of electrospun fibers was determined by the evaporation rate of the solvent. On the basis of this result, warm air was applied to increase the evaporation rate of the solvent, and the morphology and photovoltaic performance were successfully controlled under high humidity conditions. This system can enhance the reproducibility of electrospun fibers with an inexpensive apparatus, leading to the practical use of electrospinning for not only OPV devices but also for other applications.

EXPERIMENTAL SECTION

Poly(3-hexylthiophene) (P3HT; Mw 50 000; Rieke metal), poly(ethylene oxide) (PEO; Mw 900 000; Aldrich), poly(3,4-ethylenedioxythiophene):poly(styrenesulfonate) (PEDOT:PSS; Clevios P VP Al 4083, H.C. Stark), [6,6]-phenyl-C_{61}-butyric acid methyl ester (PCBM; Nano-C), chloroform (Aldrich), acetic acid (Aldrich), *N*,*N*′-dimethylformamide (DMF; Daejung, Korea), acetonitrile (Aldrich), titanium isopropoxide (Aldrich), methanol (Aldrich), and dichloromethane (Aldrich) were purchased and were used without further purification.

The electrospinning process is described in a previous paper.[11] A solution containing 0.35 wt % PEO and 0.15 wt % P3HT, dissolved in chloroform was stirred at 50 °C for 6 h. A polar cosolvent consisting of acetic acid and DMF (in a molar ratio of 2:1) was added to the solution (in a 1:8 weight ratio). The electrospinning dope solution was loaded into a syringe connected to a metal needle (gauge no. 28, inner diameter 0.18 mm) nozzle and was electrospun at a feeding rate of 1.0 mL/h in air. A bias voltage of 25 kV was applied to the metal needle, and the distance from the nozzle to the grounded collector plate was fixed at 21 cm (denoted P3HT@PEO composite nanofibers). Uniform electrospinning was achieved by reciprocating the collector glass plate and the needle nozzle using a 3-axis robot. The as-spun P3HT@PEO composite nanofibers were exposed to acetonitrile 4 times for 30 min periods to remove any PEO. Finally, virgin P3HT nanofibers were obtained. Warm air was applied to the electrospun fibers using a small heater (MFH-3615, JL Home) during the electrospinning process.

To prepare the electrospun OPV device, ITO/glass substrates were cleaned by sonication in a detergent, acetone, and isopropanol. The ITO substrates were then treated with UV/ozone for 15 min, after which PEDOT:PSS was spin-cast at 5000 rpm for 40 s. The PEDOT:PSS films were dried at 150 °C for 15 min. A 10 nm P3HT layer was then spin-coated onto the PEDOT:PSS layer as a buffer layer. P3HT@PEO composite nanofibers were directly electrospun onto the PEDOT:PSS film, and the PEO was subsequently removed using acetonitrile. A PCBM layer was spin-cast onto the active layer at 5000 rpm for 20 s from a dichloromethane solution with a concentration of 16 mg/mL. A TiO_x precursor solution was prepared as described previously.[25] The solution was spin-cast onto the top of the active layer at 5000 rpm for 40 s. A 100 nm-thick aluminum cathode was then deposited using a thermal evaporator. The devices were heat-treated at 150 °C for 30 min under a vacuum.

The morphologies of the P3HT@PEO composite nanofibers and the virgin P3HT nanofibers were examined using a field emission scanning electron microscope (FESEM; JEOL JSM-6700F) operated at an accelerating voltage of 5 kV. The photoluminescence (PL) properties were examined at an excitation wavelength of 470 nm using an LS-55 (PerkinElmer). The evaporation rate was evaluated in an electrospinning chamber based on the measured weight change. The power conversion efficiency (PCE) values of the devices were determined using a K3000 instrument (McScience).

RESULTS AND DISCUSSION

We initially investigated the effect of the RH on the morphology of electrospun fibers and the photovoltaic performance of the electrospun fibers. The photovoltaic performance was characterized on the basis of the electrospun OPV devices reported in our previous paper.[12] The structure of these devices is ITO/PEDOT:PSS/P3HT film/P3HT nanofiber/PCBM/TiO_x/Al; thus, the morphology of the P3HT nanofibers significantly influences the performances of OPV devices. The effects of humidity on the electrospinning process were explored by electrospinning the nanofibers under different ambient conditions (20%, 30%, 40%, and 50% RH).

Figure 1 shows SEM images of P3HT@PEO composite nanofibers obtained from identical spinning dope solutions.

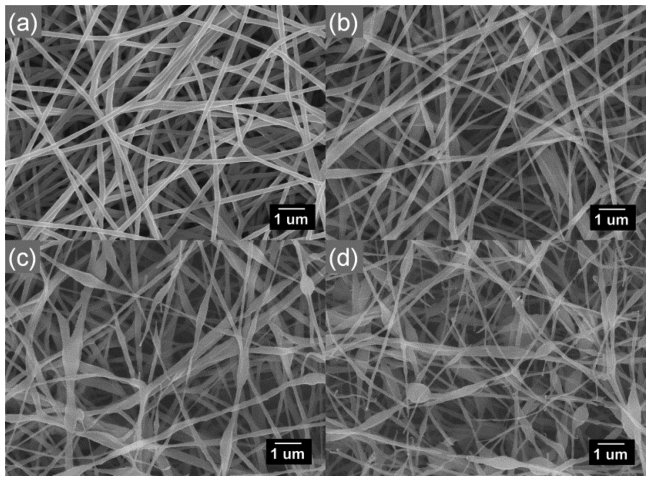

Figure 1. SEM images of electrospun P3HT@PEO composite fibers prepared at (a) 20%, (b) 30%, (c) 40%, and (d) 50% RH.

The average diameter and standard deviation of the nanofibers are summarized in Table 1 and Figure 2. The electrospun

Table 1. Variations in the Diameters of the Electrospun Fibers and Beads as a Function of the RH

RH (%)	diameter of fibers (nm)	diameter of beads (nm)
	P3HT@PEO Composite Nanofibers	
20	118.8 ± 19.5	
30	83.3 ± 18.4	186.8 ± 47.7
40	60.3 ± 26.8	241.4 ± 49.1
50	44.3 ± 13.3	301.5 ± 48.1
	P3HT Nanofibers	
20	81.2 ± 15.6	
30	63.5 ± 12.2	130.2 ± 31.1
40	49.8 ± 9.4	191.3 ± 35.9
50	38.1 ± 4.1	250.6 ± 37.7

P3HT@PEO composite fibers clearly differed in terms of their morphologies. Such a phenomenon is not only observed in PEO, a water-soluble polymer, but is also similarly observed in a water insoluble polymer, poly(ε-caprolactone) (Supporting Information Figure S2). The electrospun fibers fabricated at a higher RH tended to have a beaded morphology (shaped like "beads on a string"), and the fiber diameter tended to be thinner. We were able to investigate the morphology of the P3HT nanofiber after using acetonitrile, as presented in our previous study,[11,12] to successfully remove PEO from the

DOI: 10.1021/am508250q
ACS Appl. Mater. Interfaces 2015, 7, 4481−4487

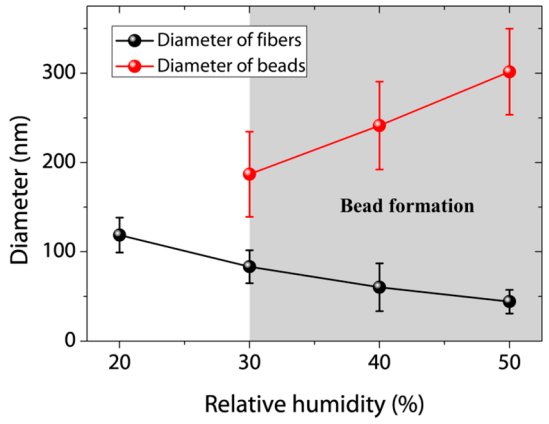

Figure 2. Variations in the diameters of the electrospun fibers and beads as a function of the RH.

P3HT@PEO composite fibers. After the PEO had been removed from the composite fibers, the beads still remained on surfaces of the fibers (Figure 3). A beaded morphology can

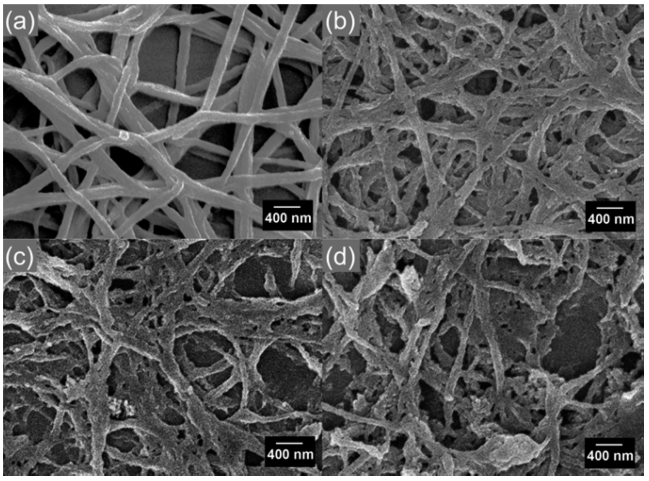

Figure 3. SEM images of electrospun P3HT fibers prepared at (a) 20%, (b) 30%, (c) 40%, and (d) 50% RH.

be useful in some applications, but it was undesirable for the OPV cells prepared here. The average diameters of some of the beads on the fibers prepared at 50% RH exceeded 300 nm and were thicker than the active layer of the OPV device. The beads on the P3HT fibers would act as an aggregation region of the active layer. Aggregated regions in a bulk heterojunction structure reportedly reduce the efficiency of the cell.[26] Reducing the humidity was found to help reduce the number and size of the beads. These beads were not observed in electrospun fibers prepared at 20% RH.

We have investigated the degree of crystallinity of the obtained P3HT nanofibers in order to eliminate the possible change in the performance of OPV devices due to a decrease induced by the degree of crystallinity other than morphology. Consistency in the degree of crystallinity was seen regardless of humidity (Supporting Information Figure S3), showing that the morphology of P3HT nanofibers have a direct relationship with the performance of the OPV device.

As a feasibility test of OPV devices, the PL test is an appropriate method with which to check for successful exciton dissociation. When excitons successfully are diffused to the interface between P3HT fibers and PCBM, the excitons are dissociated and PL is not observed. However, if the P3HT fibers are too thick to be diffused onto the interface, the excitons will be recombined and generate PL. The beadless P3HT fibers and beaded P3HT fibers would show the different exciton dissociation behavior. We spin-cast a PCBM layer onto P3HT fibers prepared under two conditions (20% RH and 50% RH) and examined the PL properties to observe the exciton dissociation. Figure 4 shows the PL of the P3HT fiber and the

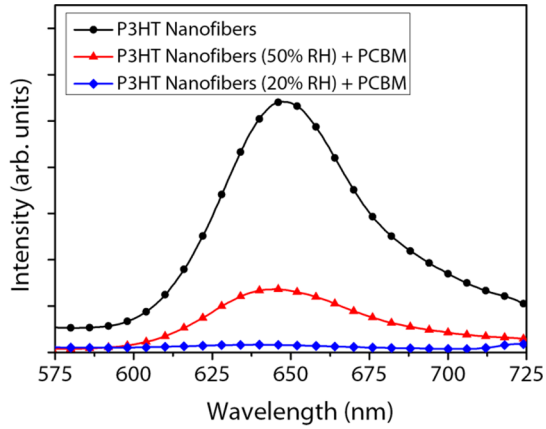

Figure 4. PL properties of the virgin P3HT nanofibers and the composite films composed of PCBM and virgin P3HT nanofibers.

P3HT fiber/PCBM films. The P3HT showed a PL peak at 650 nm which was quenched after PCBM was coated onto the P3HT nanofibers. This is evidence of successful exciton dissociation in P3HT nanofibers. However, the P3HT nanofibers prepared at 50% RH still showed PL after the PCBM coating process. Due to the large diameter of the beads, some excitons recombined before diffusing into the interface between P3HT and PCBM. This result indicated that morphology of the P3HT nanofibers influenced the exciton dissociation state.

Because the above PL and SEM results show that the change in humidity induces the morphological change in the P3HT electrospun nanofibers and because such morphological change affects the exciton dissociation behavior, it can be predicted that P3HT electrospun nanofiber based OPV devices will also show a change in performance according to the humidity exposed. Before fabricating nanofiber based OPV devices, it is necessary to examine if humidity gives any other influences to the OPV device. For example, water vapor molecule could induce material degradation or oxidation of the electrode.[27] In order to observe the reason for decrease in the device performance, bilayer devices composed of P3HT/PCBM were fabricated and was investigated whether humidity is an influence to the device. Other than being topped with a spin-cast P3HT film instead of an electrospun P3HT nanofiber, such bilayer devices share the same fabrication condition with electrospun OPV devices, fabricated in air atmosphere of 20% RH and 50% RH. The two bilayer-structured OPV devices showed similar performance levels (Supporting Information Figure S1). This result suggests that, for general reference OPV devices, the humidity in the fabrication process does not affect the performance significantly. In other words, if electrospun OPV devices fabricated at various humidity conditions show a different performance, then it means that it is solely caused the morphological change of electrospun P3HT nanofibers.

DOI: 10.1021/am508250q
ACS Appl. Mater. Interfaces 2015, 7, 4481−4487

The effects of the fiber morphology on the performances of OPV devices prepared from electrospun P3HT nanofibers fabricated under the ambient conditions listed in Table 2 were explored. The power conversion efficiency was found to be inversely related to the RH (Figure 5). The J_{SC} and fill factor (FF) values of the OPV devices depended significantly on the RH. Poor exciton dissociation and recombination from the large beads can lead to poor J_{SC} and FF values. These experimental results indicate that the performances of the electrospun OPV devices depended on the ambient conditions because the morphologies of the electrospun fibers were quite sensitive to the RH.

Table 2. Performances of the OPV Devices Prepared Using P3HT Nanofibers with Various Diameters

RH (%)	V_{OC} (V)	J_{SC} (mA/cm^2)	FF	PCE (%)
20	0.604	7.00	50.2	2.12
30	0.546	5.12	45.0	1.26
40	0.497	4.01	37.7	0.75
50	0.439	2.19	30.9	0.30

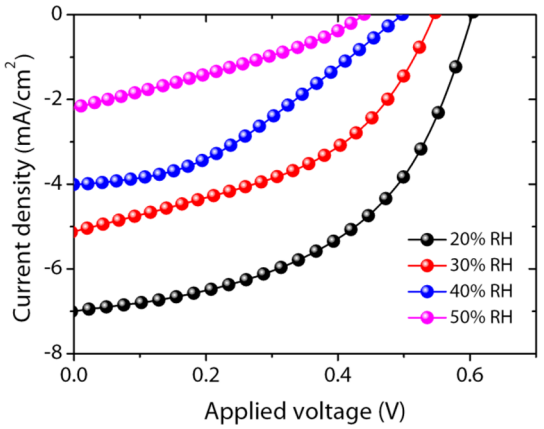

Figure 5. J–V curves obtained from the electrospun OPV devices prepared from the P3HT nanofibers fabricated at 20%, 30%, 40%, and 50%.

Previous studies reported that electrospun fibers prepared under high RH conditions display small-diameter fibers,[22] large-diameter fibers,[20] porous surfaces,[20] or a fused morphology.[19] On the other hand, the high humidity conditions applied in the present study resulted in the preparation of beaded electrospun nanofibers with small diameters. Furthermore, previous studies discussed the effect of the humidity level on an aqueous solution system, which is an inappropriate description for the system in this work. Because RH is defined as the ratio of the amount of water vapor in the air to the saturating amount of water in the air at a specific temperature, a high partial pressure of water vapor in the air at a high humidity can prevent the evaporation of water during electrospinning. Slow evaporation is thought to allow a water-based spinning dope solution sufficient time to stretch, thereby producing fibers with small diameters. On the other hand, a longer stretching time could provide time to form beads due to Rayleigh instabilities in the solution. A small fiber diameter and the formation of beads appear to be inseparable features of the electrospinning technique. The experimental results in this study supported these general principles.

The discussion presented in the previous section relied on the fact that the water evaporation rate depends on the humidity; however, the solvent used in the electrospinning system discussed here was chloroform. It was not clear whether the evaporation rates of solvents other than water were affected by the RH. Because RH is a value defined by the amount of water vapor, it is necessary to verify whether the water vapor affects the evaporation rate of other solvents. Nevertheless, alcohol-based spinning dope solutions have been known to spin fibers with small diameters at a high RH,[22] suggesting that the alcohol evaporation rate is also influenced by the RH. Changes in the alcohol evaporation rate may be induced by the adsorption of water molecules to the surface of the alcohol at high humidities.[28] The adsorption of water molecules may also occur on surface of the chloroform solution, thereby preventing the evaporation of the chloroform. To the best of our knowledge, the RH-dependent chloroform evaporation rate has not previously been investigated. We therefore measured the evaporation rates of water, ethanol, and chloroform under different RH conditions to investigate the effects of RH on the three solvents. Table 3 and Figure 6 present the evaporation rates of the three solvents at 20, 30, 40, and 50% RH. Because the vapor pressure of the chloroform is smaller than that of ethanol and water, chloroform showed the highest evaporation rate under all conditions. The high chloroform evaporation rate formed beadless electrospun fibers from a low spinning dope solution concentration (~0.35 wt %). A humidity-dependent evaporation rate was observed for both chloroform and ethanol, as well as for water. All solvents examined in this experiment exhibited low evaporation rates under high RH conditions. These results indicated that the water molecules in the ambient atmosphere prevented the evaporation of water as well as other solvents. These results suggested that high humidity conditions provide spinning dope solutions ample time for stretching and/or bead formation before the fiber morphology sets (Scheme

Table 3. Variations in the Solvent Evaporation Rate under Different RH Conditions

RH (%)	chloroform (g/s m^2)	ethanol (g/s m^2)	water (g/s m^2)
20	0.829 ± 0.036	0.189 ± 0.006	0.0364 ± 0.0025
30	0.684 ± 0.024	0.146 ± 0.005	0.0303 ± 0.0021
40	0.655 ± 0.026	0.138 ± 0.005	0.0271 ± 0.0027
50	0.644 ± 0.020	0.133 ± 0.005	0.0246 ± 0.0029

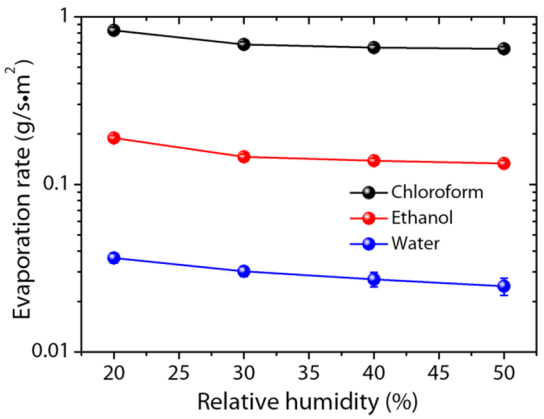

Figure 6. Variations in the solvent evaporation rate under different RH conditions.

DOI: 10.1021/am508250q
ACS Appl. Mater. Interfaces 2015, 7, 4481−4487

1a). This effect is observed for both aqueous and nonaqueous dope solutions.

Scheme 1. (a) Schematic of Electrospinning Process under Low (left) and High (right) RH and (b) under a Heater System

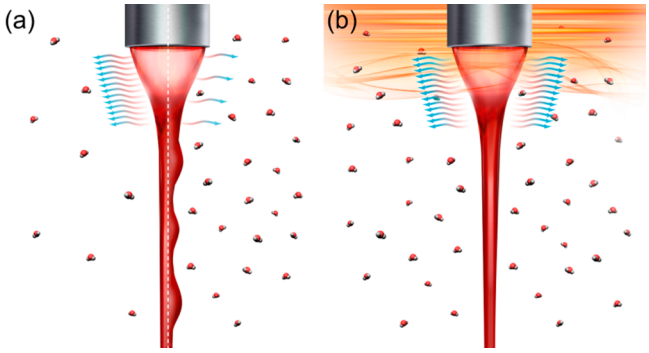

Some studies have reported that the diameters of electrospun fibers fabricated under high humidity conditions are consistently small with uniform morphologies.[22] In this experiment, however, both the diameter and morphology of the fibers were observed to differ under low and high RH conditions. A 0.35 wt % dope solution was a critical concentration for the creation of a beadless morphology; therefore, slight changes in the conditions may induce significant morphological changes. Indeed, fibers electrospun from a 0.5 wt % PEO solution formed few beads on the fibers, even at a high RH (Supporting Information Figure S4), despite the longer drying time, because the high viscosity of the 0.5 wt % PEO solution (21.09 cP) compared with the 0.35 wt % solution (9.53 cP) resisted the formation of beads. Highly concentrated spinning dope solutions are generally not appropriate for the preparation of nanofibers.

The high-RH conditions reduce the solvent evaporation rate and enable the generation of beads on the electrospun fibers. A high evaporation rate is necessary for the production of bead-free electrospun fibers; however, expensive systems are required for the maintenance of a very low RH (<20%) during a humid season, thereby undercutting one of the primary merits of the electrospinning technique. Blowing warm air across the fibers during electrospinning provides an alternative method for increasing the evaporation rate of the solvent. Heated air streams have been used in conventional dry spinning systems to induce the rapid evaporation of solvents. We simply directed warm air (50 °C) over the electrospinning system using a small heater and increased the evaporation rate of the chloroform to 2.15 g/s m^2. This rate exceeded the evaporation rate obtained at 20% RH, suggesting that the beadless morphology may be achieved under high humidity conditions using a facile and inexpensive system. Figure 7 shows the morphologies of the electrospun fibers fabricated using the heater under high humidity conditions. The beads were completely absent from the fiber surfaces, and the average fiber diameter was similar to the diameters of fibers obtained at 20% RH. This result clearly indicated that the simple heating system can address the poor reproducibility of the electrospinning technique under high humidity conditions. A schematic of rapid evaporation and formation of beadless fibers under a heater system is illustrated in Scheme 1b.

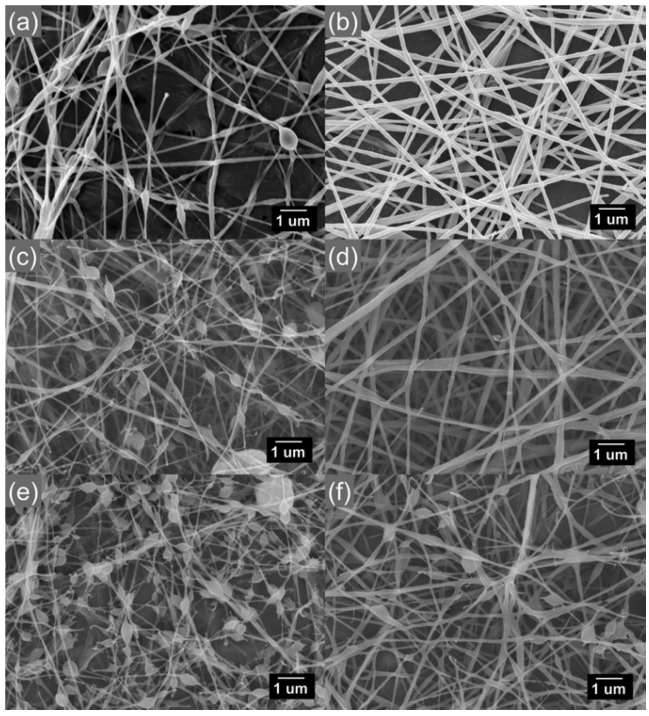

Figure 7. SEM micrographs of the P3HT@PEO composite fibers prepared from spinning dope solutions having (a, b) 0.35 wt % PEO concentrations at 50% RH, and (c, d) 0.3 wt %, or (e, f) 0.25 wt % PEO concentrations at 20% RH, under a heater system (b, d, f) or without the system (a, c, e).

We assumed that the slow solvent evaporation rate under high RH conditions provided ample time for the formation of beads due to the Rayleigh fluid instabilities. If this assumption were correct, the high evaporation rate achieved using the heater system was expected to prevent the formation of beads on the electrospun fibers prepared from spinning dope solutions with concentrations lower than 0.35 wt %, which marks the concentration threshold for transitioning from beadless (concentrations exceeding 0.35 wt %) to beaded (concentrations less than 0.35 wt %, Figure 7c,e) fibers at 20% RH. Indeed, beads formed on the fibers electrospun from 0.3 and 0.25 wt % solutions but were absent or reduced from the fibers prepared from the same solutions under the application of the heater system (see Figure 7d,f). The concentration threshold for bead formation depended sensitively on the evaporation behavior and could be controlled through systematic tuning. This approach has practical significance for fibers prepared from spinning dope solutions having low concentrations as a result of other processing constraints, such as limited polymer solubility.

OPV devices prepared using the electrospun fibers were tested to measure the influence of the morphological changes on the OPV performance. The nanofibrous OPV devices prepared using the heater system and the OPV devices prepared at 20% RH exhibited similar performances (Figure 8). Figure 8 clearly indicates that the heater system successfully recovered the device performance. Application of the heater system under high humidity conditions increased the J_{SC} and power conversion efficiency from 2.19 mA/cm^2 and 0.30% to 7.01 mA/cm^2 and 2.07%, respectively. In order to check if the change in the degree of crystallinity is influenced by the heater, the structural characteristics of P3HT fiber electrospun under

DOI: 10.1021/am508250q
ACS Appl. Mater. Interfaces 2015, 7, 4481−4487

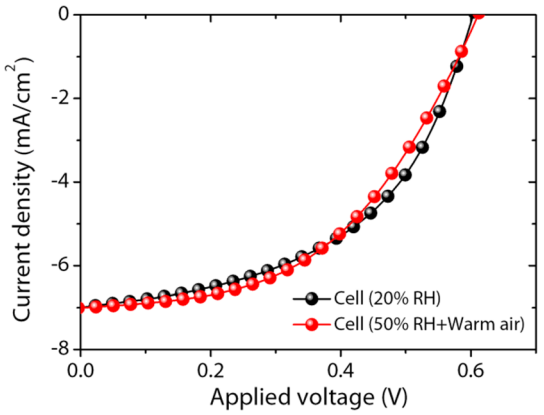

Figure 8. $J-V$ curves obtained from the electrospun OPV devices prepared from the P3HT nanofibers prepared at 20% RH or with heating system at 50% RH.

the heater system were analyzed (Supporting Information Figure S3). Practically, hot air flow is not applied to the deposited electrospun fiber continuously, but is rather only applied during spinning; therefore, it does not affect the crystallinity greatly. The method proposed in this study successfully recovered the morphology of the electrospun fibers and their photovoltaic performances as listed in Table 4. It should be noted that the effects of the active layer P3HT morphology on the photovoltaic performance might also be investigated using the application of heat as a means for controlling the morphology. This system may be applied to any application that relies on electrospun fibers, to improve the reproducibility or prepare bead-free fibers under high humidity conditions.

CONCLUSIONS

We investigated the effects of the humidity on the morphologies of electrospun fibers and the performance of OPV devices. A high humidity was found to reduce the solvent evaporation rate, whether the solvent was chloroform or water. Low evaporation rates induced Rayleigh instabilities that generated beads on the surfaces of the electrospun fibers. OPV devices prepared using beaded fibers exhibited a poor device efficiency due to low J_{SC} and FF values. The application of warm air onto the electrospinning system during operation enhanced the solvent evaporation rate and prevented the formation of beads on the electrospun fibers. OPV devices prepared using the beadless P3HT nanofibers displayed high J_{SC}, FF, and power conversion efficiencies.

The results of this study revealed that the evaporation rate depended on the ambient conditions and significantly influenced the morphology of the electrospun fibers, thereby reducing the reproducibility of the method. The heating method proposed here is simple, inexpensive, and effective for recovering the beadless morphologies of electrospun fibers, even under high humidity conditions, by increasing the evaporation rate. Most importantly, this system can be used in both OPV devices and in OTFTs, sensors, and other applications employing electrospun nanofibers.

ASSOCIATED CONTENT

Supporting Information

Additional data on $J-V$ curve and SEM images. This material is available free of charge via the Internet at http://pubs.acs.org.

AUTHOR INFORMATION

Corresponding Author

*E-mail: crpark@snu.ac.kr.

Notes

The authors declare no competing financial interest.

ACKNOWLEDGMENTS

This research was supported by the Midcareer Researcher Program through the National Research Foundation of Korea, funded by the Ministry of Science, ICT & Future Planning (No. 2010-0029244).

REFERENCES

(1) Greiner, A.; Wendorff, J. H. Electrospinning: A Fascinating Method for the Preparation of Ultrathin Fibers. *Angew. Chem., Int. Ed.* **2007**, *46*, 5670−5703.

(2) Hou, H.; Jun, Z.; Reuning, A.; Schaper, A.; Wendorff, J. H.; Greiner, A. Poly(p-Xylylene) Nanotubes by Coating and Removal of Ultrathin Polymer Template Fibers. *Macromolecules* **2002**, *35*, 2429−2431.

(3) Mahanta, N.; Valiyaveettil, S. Surface Modified Electrospun Poly(Vinyl Alcohol) Membranes for Extracting Nanoparticles from Water. *Nanoscale* **2011**, *3*, 4625−4631.

(4) Choi, H. S.; Im, J. H.; Kim, T.; Park, J. H.; Park, C. R. Advanced Energy Storage Device: A Hybrid Batcap System Consisting of Battery-Supercapacitor Hybrid Electrodes Based on Li4Ti5O12-Activated-Carbon Hybrid Nanotubes. *J. Mater. Chem.* **2012**, *22*, 16986−16993.

(5) Wang, S.-X.; Yang, L.; Stubbs, L. P.; Li, X.; He, C. Lignin-Derived Fused Electrospun Carbon Fibrous Mats as High Performance Anode Materials for Lithium Ion Batteries. *ACS Appl. Mater. Interfaces* **2013**, *5*, 12275−12282.

(6) Im, J. H.; Yang, S. J.; Yun, C. H.; Park, C. R. Simple Fabrication of Carbon/TiO2 Composite Nanotubes Showing Dual Functions with Adsorption and Photocatalytic Decomposition of Rhodamine B. *Nanotechnology* **2012**, *23*, 035604.

(7) Chang, H.-C.; Liu, C.-L.; Chen, W.-C. Flexible Nonvolatile Transistor Memory Devices Based on One-Dimensional Electrospun P3HT:Au Hybrid Nanofibers. *Adv. Funct. Mater.* **2013**, *23*, 4960−4968.

(8) Lee, S.; Moon, G. D.; Jeong, U. Continuous Production of Uniform Poly(3-Hexylthiophene) (P3HT) Nanofibers by Electrospinning and Their Electrical Properties. *J. Mater. Chem.* **2009**, *19*, 743−748.

(9) Mao, X.; Simeon, F.; Rutledge, G. C.; Hatton, T. A. Electrospun Carbon Nanofiber Webs with Controlled Density of States for Sensor Applications. *Adv. Mater.* **2013**, *25*, 1309−1314.

(10) Zhang, Z.; Li, X.; Wang, C.; Wei, L.; Liu, Y.; Shao, C. ZnO Hollow Nanofibers: Fabrication from Facile Single Capillary Electro-

Table 4. Performance Properties of the OPV Devices Prepared Using P3HT Nanofibers with Various Diameters

	V_{OC} (V)	J_{SC} (mA/cm^2)	FF	PCE (%)
cell (20% RH)	0.603 (0.600 ± 0.010)[a]	7.00 (6.64 ± 0.41)	50.2 (51.1 ± 2.3)	2.12 (2.03 ± 0.10)
cell (50% RH + warm air)	0.611 (0.602 ± 0.014)	7.01 (6.71 ± 0.31)	48.5 (50.0 ± 1.3)	2.07 (2.02 ± 0.07)

[a]Numbers in parentheses indicate average values.

DOI: 10.1021/am508250q
ACS Appl. Mater. Interfaces 2015, 7, 4481−4487

spinning and Applications in Gas Sensors. *J. Phys. Chem. C* **2009**, *113*, 19397−19403.
(11) Kim, T.; Im, J. H.; Choi, H. S.; Yang, S. J.; Kim, S. W.; Park, C. R. Preparation and Photoluminescence (PL) Performance of a Nanoweb of P3ht Nanofibers with Diameters Below 100 nm. *J. Mater. Chem.* **2011**, *21*, 14231−14239.
(12) Kim, T.; Yang, S. J.; Kim, S. K.; Choi, H. S.; Park, C. R. Preparation of PCDTBT Nanofibers with a Diameter of 20 nm and Their Application to Air-Processed Organic Solar Cells. *Nanoscale* **2014**, *6*, 2847−2854.
(13) Park, H.; Chang, S.; Jean, J.; Cheng, J. J.; Araujo, P. T.; Wang, M.; Bawendi, M. G.; Dresselhaus, M. S.; Bulović, V.; Kong, J.; Gradečak, S. Graphene Cathode-Based ZnO Nanowire Hybrid Solar Cells. *Nano Lett.* **2012**, *13*, 233−239.
(14) Yu, M.; Long, Y.-Z.; Sun, B.; Fan, Z. Recent Advances in Solar Cells Based on One-Dimensional Nanostructure Arrays. *Nanoscale* **2012**, *4*, 2783−2796.
(15) Coakley, K. M.; Srinivasan, B. S.; Ziebarth, J. M.; Goh, C.; Liu, Y. X.; McGehee, M. D. Enhanced Hole Mobility in Regioregular Polythiophene Infiltrated in Straight Nanopores. *Adv. Funct. Mater.* **2005**, *15*, 1927−1932.
(16) Treat, N. D.; Varotto, A.; Takacs, C. J.; Batara, N.; Al-Hashimi, M.; Heeney, M. J.; Heeger, A. J.; Wudl, F.; Hawker, C. J.; Chabinyc, M. L. Polymer-Fullerene Miscibility: A Metric for Screening New Materials for High-Performance Organic Solar Cells. *J. Am. Chem. Soc.* **2012**, *134*, 15869−15879.
(17) Tremolet de Villers, B.; Tassone, C. J.; Tolbert, S. H.; Schwartz, B. J. Improving the Reproducibility of P3HT:PCBM Solar Cells by Controlling the PCBM/Cathode Interface. *J. Phys. Chem. C* **2009**, *113*, 18978−18982.
(18) Ye, L.; Jing, Y.; Guo, X.; Sun, H.; Zhang, S.; Zhang, M.; Huo, L.; Hou, J. Remove the Residual Additives toward Enhanced Efficiency with Higher Reproducibility in Polymer Solar Cells. *J. Phys. Chem. C* **2013**, *117*, 14920−14928.
(19) Vrieze, S.; Camp, T.; Nelvig, A.; Hagström, B.; Westbroek, P.; Clerck, K. The Effect of Temperature and Humidity on Electrospinning. *J. Mater. Sci.* **2009**, *44*, 1357−1362.
(20) Huang, L.; Bui, N.-N.; Manickam, S. S.; McCutcheon, J. R. Controlling Electrospun Nanofiber Morphology and Mechanical Properties Using Humidity. *J. Polym. Sci., Part B: Polym. Phys.* **2011**, *49*, 1734−1744.
(21) Htike, H. H.; Long, C.; Sukigara, S. The Effect of Relative Humidity on Electrospinning of Poly-(Vinyl Alcohol) with Soluble Eggshell Membrane. *J. Text. Eng.* **2012**, *58*, 9−12.
(22) Cai, Y.; Gevelber, M. The Effect of Relative Humidity and Evaporation Rate on Electrospinning: Fiber Diameter and Measurement for Control Implications. *J. Mater. Sci.* **2013**, *48*, 7812−7826.
(23) Guo, S.; Herzig, E. M.; Naumann, A.; Tainter, G.; Perlich, J.; Müller-Buschbaum, P. Influence of Solvent and Solvent Additive on the Morphology of PTB7 Films Probed via X-Ray Scattering. *J. Phys. Chem. B* **2013**, *118*, 344−350.
(24) Müller-Buschbaum, P. The Active Layer Morphology of Organic Solar Cells Probed with Grazing Incidence Scattering Techniques. *Adv. Mater.* **2014**, *26*, 7692−7709.
(25) Park, S. H.; Roy, A.; Beaupre, S.; Cho, S.; Coates, N.; Moon, J. S.; Moses, D.; Leclerc, M.; Lee, K.; Heeger, A. J. Bulk Heterojunction Solar Cells with Internal Quantum Efficiency Approaching 100%. *Nat. Photonics* **2009**, *3*, 297−303.
(26) Hoppe, H.; Glatzel, T.; Niggemann, M.; Schwinger, W.; Schaeffler, F.; Hinsch, A.; Lux-Steiner, M. C.; Sariciftci, N. S. Efficiency Limiting Morphological Factors of MDMO-PPV:PCBM Plastic Solar Cells. *Thin Solid Films* **2006**, *511−512*, 587−592.
(27) Kim, T.; Kang, J. H.; Yang, S. J.; Sung, S. J.; Kim, Y. S.; Park, C. R. Facile Preparation of Reduced Graphene Oxide-Based Gas Barrier Films for Organic Photovoltaic Devices. *Energy Envion. Sci.* **2014**, *7*, 3403−3411.
(28) Innocenzi, P.; Malfatti, L.; Costacurta, S.; Kidchob, T.; Piccinini, M.; Marcelli, A. Evaporation of Ethanol and Ethanol−Water Mixtures Studied by Time-Resolved Infrared Spectroscopy. *J. Phys. Chem. A* **2008**, *112*, 6512−6516.

DOI: 10.1021/am508250q
ACS Appl. Mater. Interfaces 2015, 7, 4481−4487